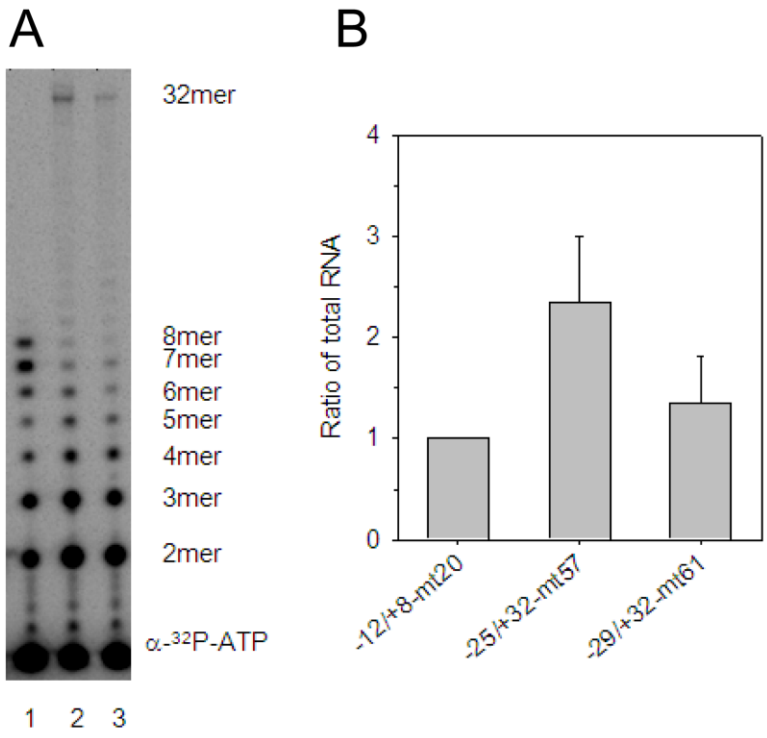

Supplementary Figure S1. In-vitro transcription on the promoter template.

(A) Transcription reaction was performed at 25°C with 4 μM DNA, 3 μM Rpo41-Mtf1, 100 μM ATP, and 250 μM each of GTP, UTP, and CTP, spiked with α-^{32}P-ATP. Lanes show the RNA products resolved on a sequencing gel. Lanes 1, 2, and 3 are for the 20-bp promoter DNA (-12/+8-mt20), -25/+32-mt57, and -29/+32-mt61, respectively. The DNA sequence (non-template strand) for -25/+32-mt57 is 5'-ATAATTTATTTATTATTATATAAGTAATAAATAATTGTTTTAT ATAATAAGAATTCC and for -29/+32-mt61 is 5'-GGCCATAATTTATTTATTATTATATAAGTA ATAAATAATTGTTTTATATAATAAGAATTCC.

(B) Comparison of the efficiency of ATP converted to RNA. Total RNA from 2- to 8-mer for the 20-bp DNA (-12/+8-mt20) was compared to those from 2- to 32-mer for the longer DNA templates.

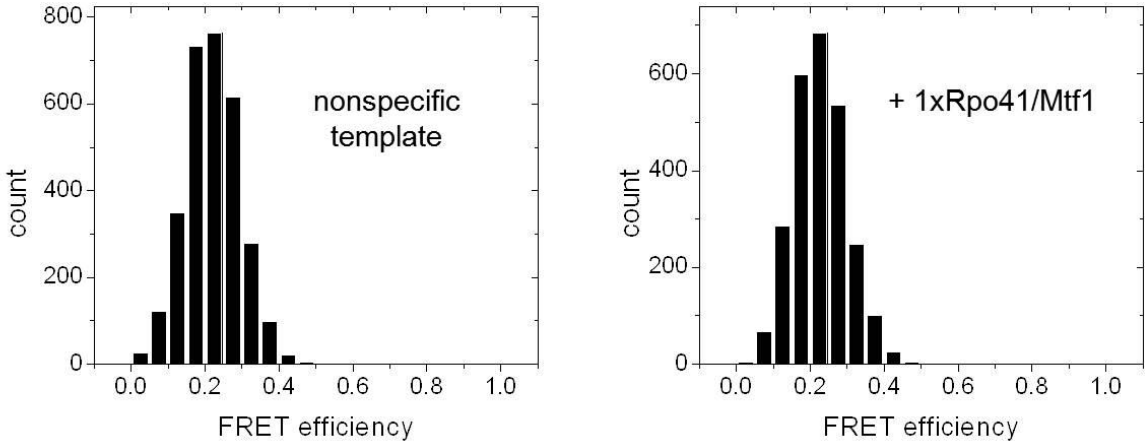


```
Random20A strand 5′-TAMRA-TAGCGTACTAGCAGCGAAGT-3′
Random20B strand       3′-ATCGCATGATCGTCGCTTCA-Alexa647-5′
```

Supplementary Figure S2. DNA template with randomly generated sequence does not show any FRET change when encapsulated with the stoichiometric amount of Rpo41-Mtf1.

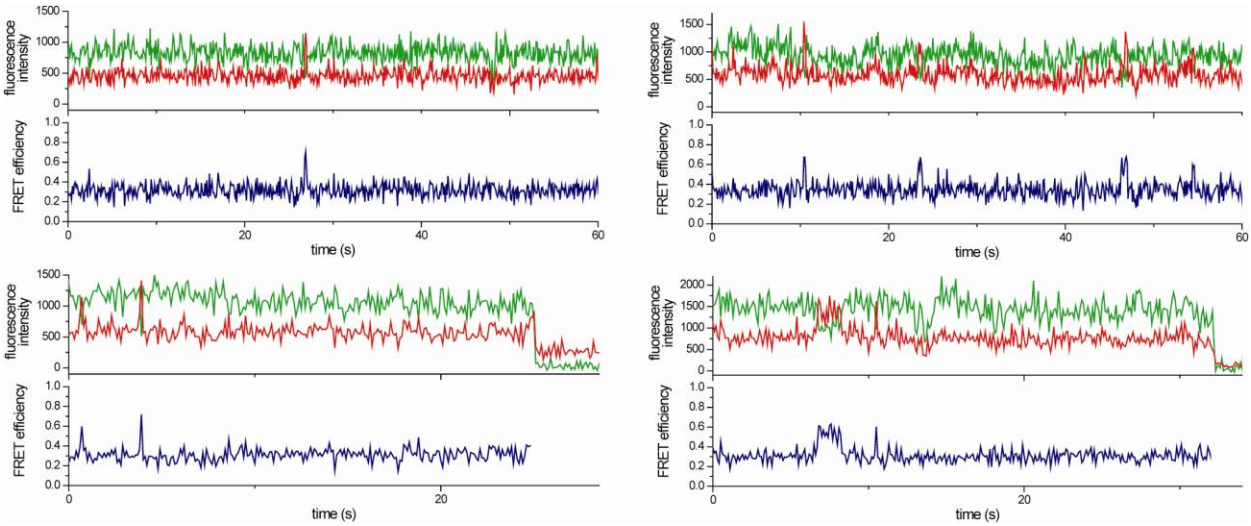

Supplementary Figure S3. Examples of single molecule traces exhibiting promoter opening trials by Rpo41 alone

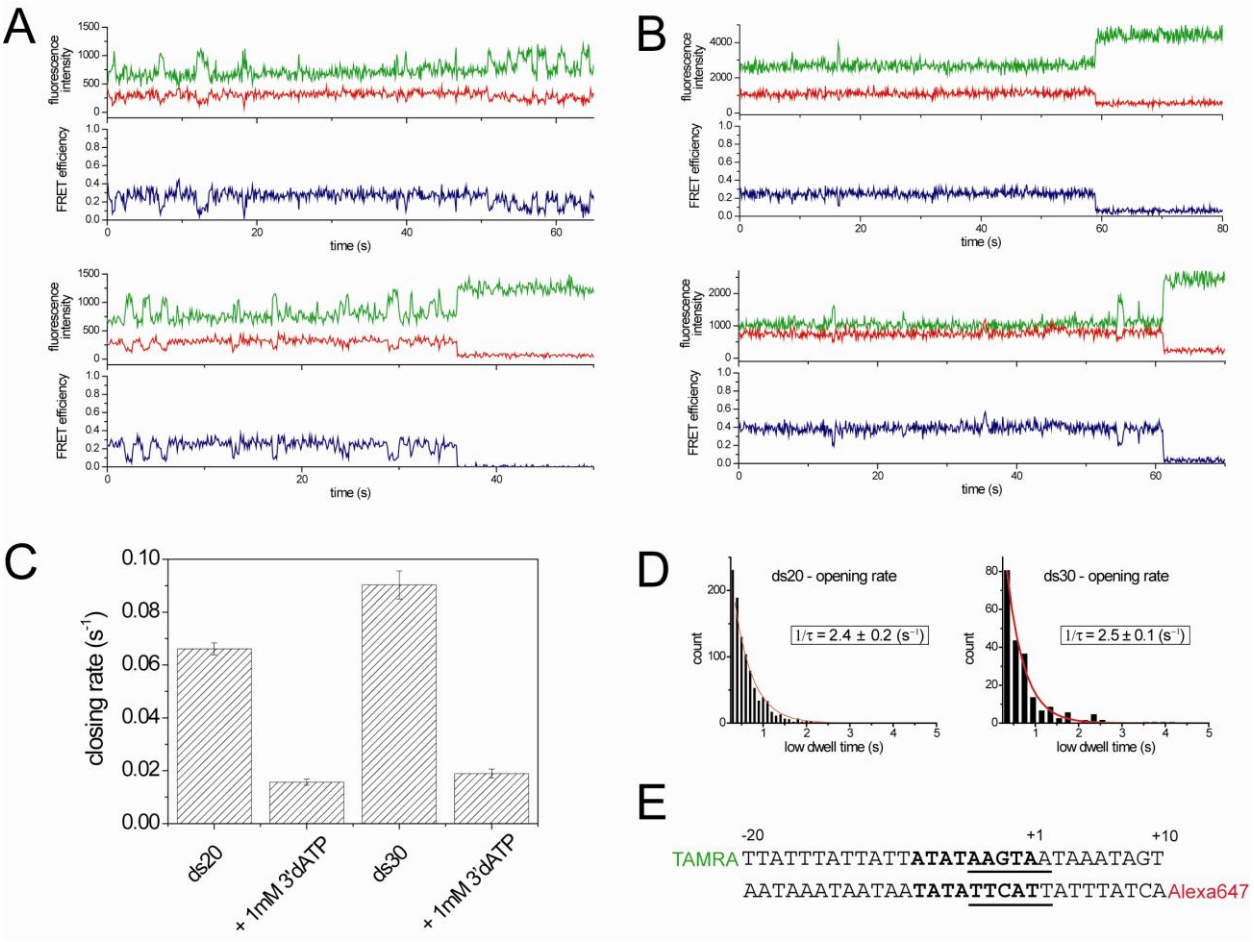

Supplementary Figure S4. Opening-closing dynamics of 30-mer template

(A) Example traces of 30-mer template bound with Rpo41/Mtf1, exhibiting similar dynamics with 20-mer template.

(B) Addition of 1 mM 3'-dATP suppresses the fluctuation as it does for 20-mer template.

(C) 20-mer and 30-mer templates give similar closing rates with or without 3'-dATP.

(D) 20-mer and 30-mer templates give almost same opening rates without 3'-dATP.

(E) Design of the 30-mer template with longer flanking sequences at both ends.

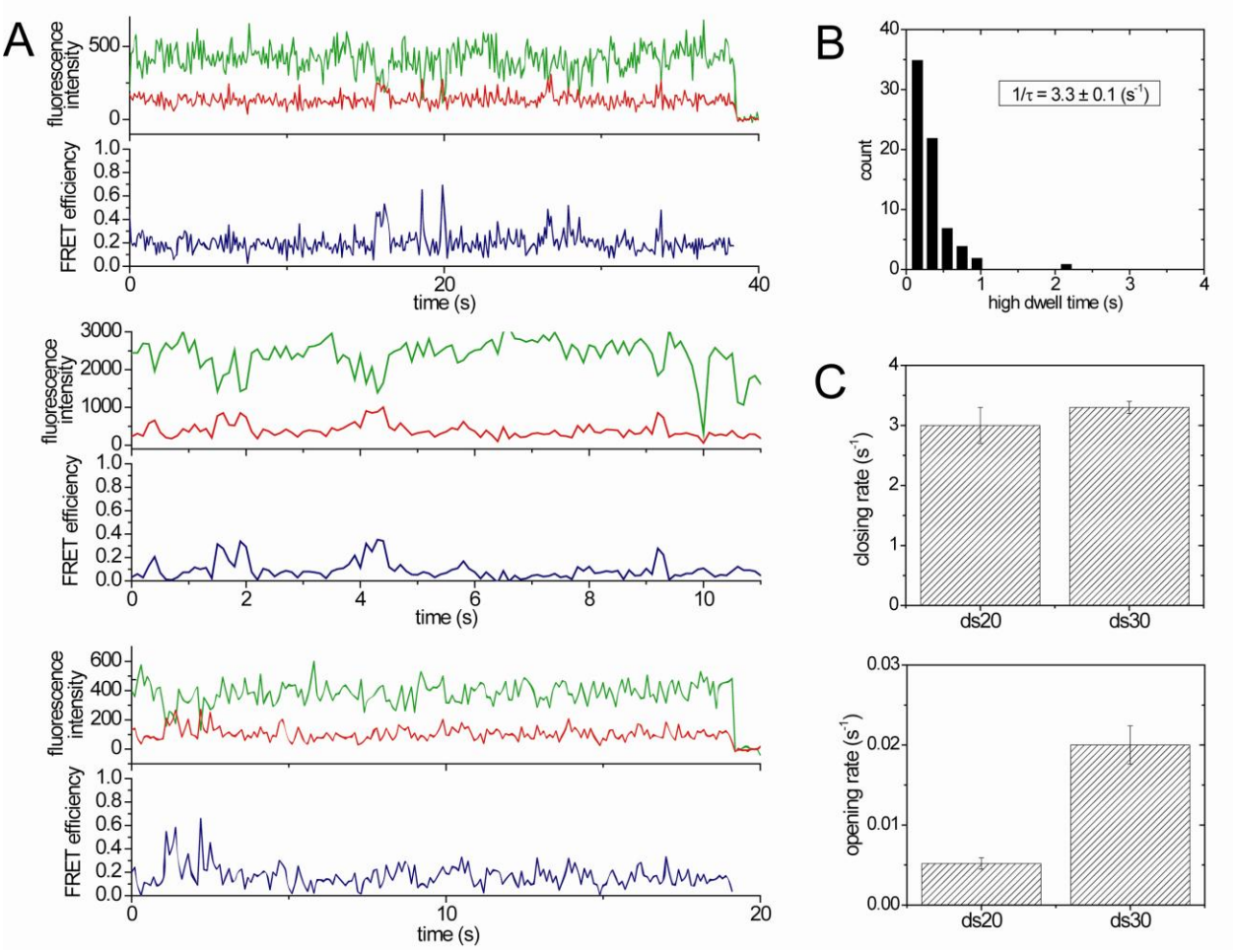

Supplementary Figure S5. Opening-closing dynamics of 30-mer template with Rpo41 alone

(A) Example traces showing promoter-opening trials by Rpo41 alone. 10x concentration of Rpo41 was co-encapsulated with the DNA template.

(B) Closing rate was estimated from the dwell times at the high FRET state.

(C) Closing rate is comparable to that of the short template. Opening rate is higher for the longer template possibly due to multiple Rpo41 interacting with one template.

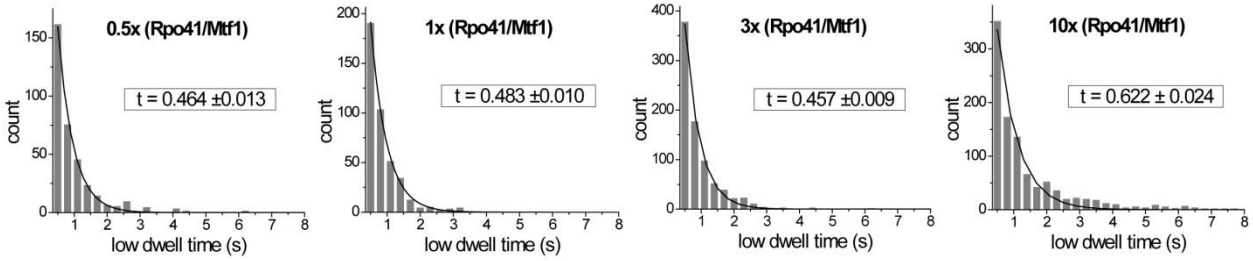

Supplementary Figure S6. Distribution of low FRET dwell time at different ratios of protein/DNA mixing. There is no significant change up to 3x, while slight increase was observed at 10x, possibly due to multiple polymerases interacting with one template.

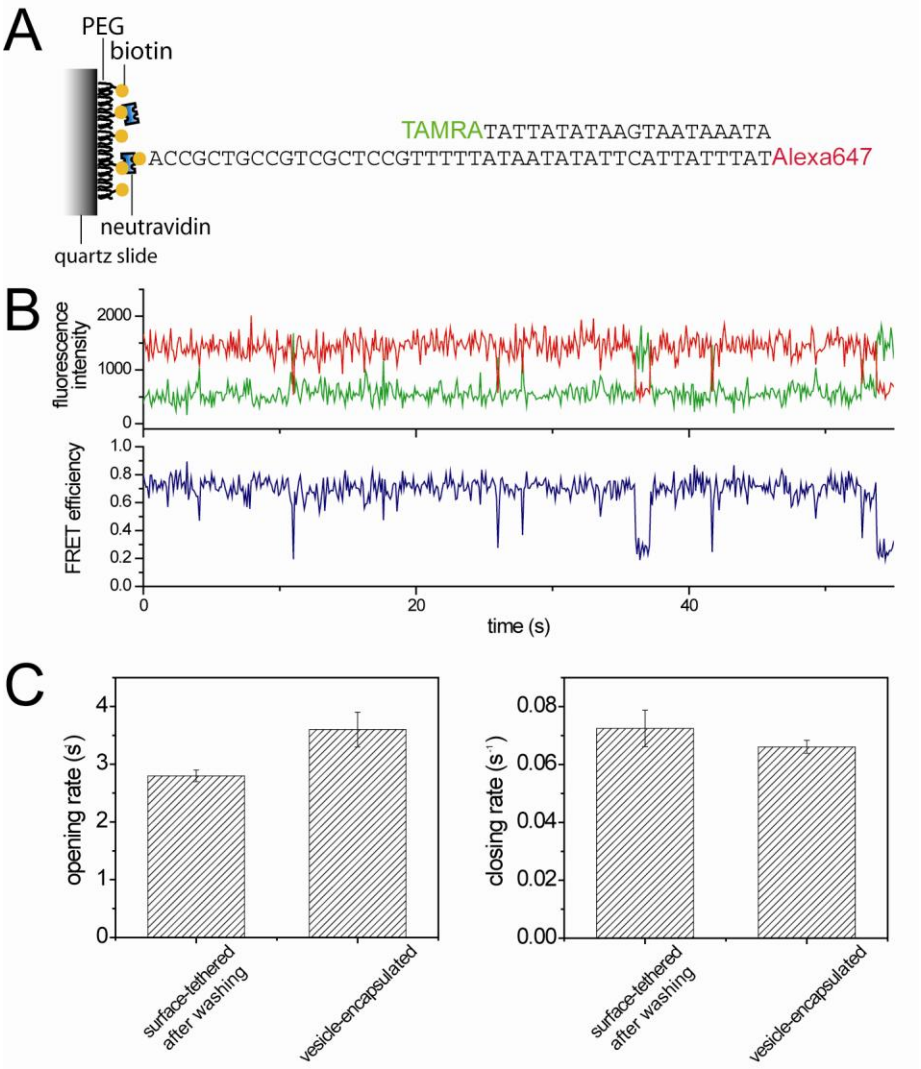

Supplementary Figure S7. Opening-closing dynamics observed with surface-tethered template after washing away free proteins in solution

(A) Schematic of surface-tethered template.

(B) Example trace after washing away free proteins in the buffer. Without proteins present in the buffer, the open complex still exhibits the same fluctuating behavior.

(C) Comparison of the transition rates between surface-tethered template after washing and vesicle-encapsulated template.

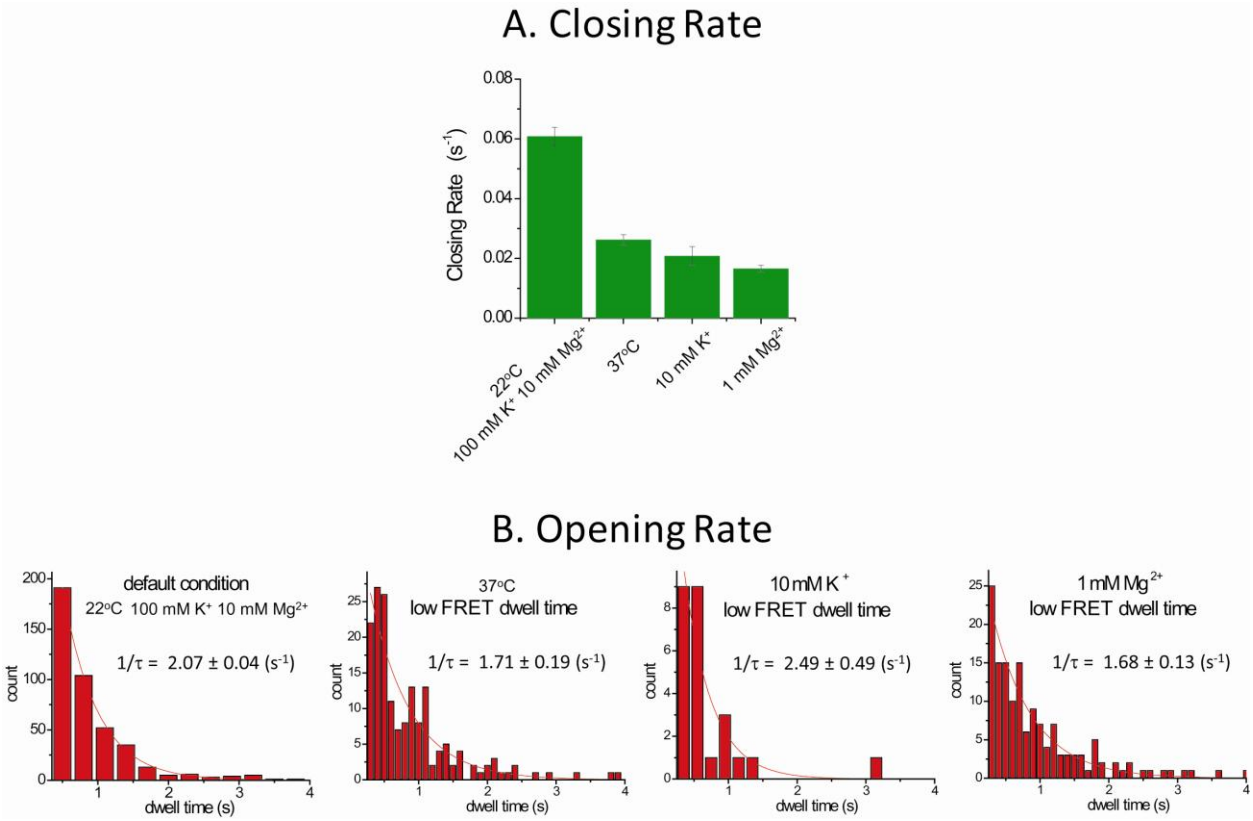

Supplementary Figure S8. Effect of temperature and salt concentration on the transition rates

(A) Change of the closing rate upon increasing temperature or decreasing salt concentrations.

(B) Comparison of the opening rate which does not show significant difference.

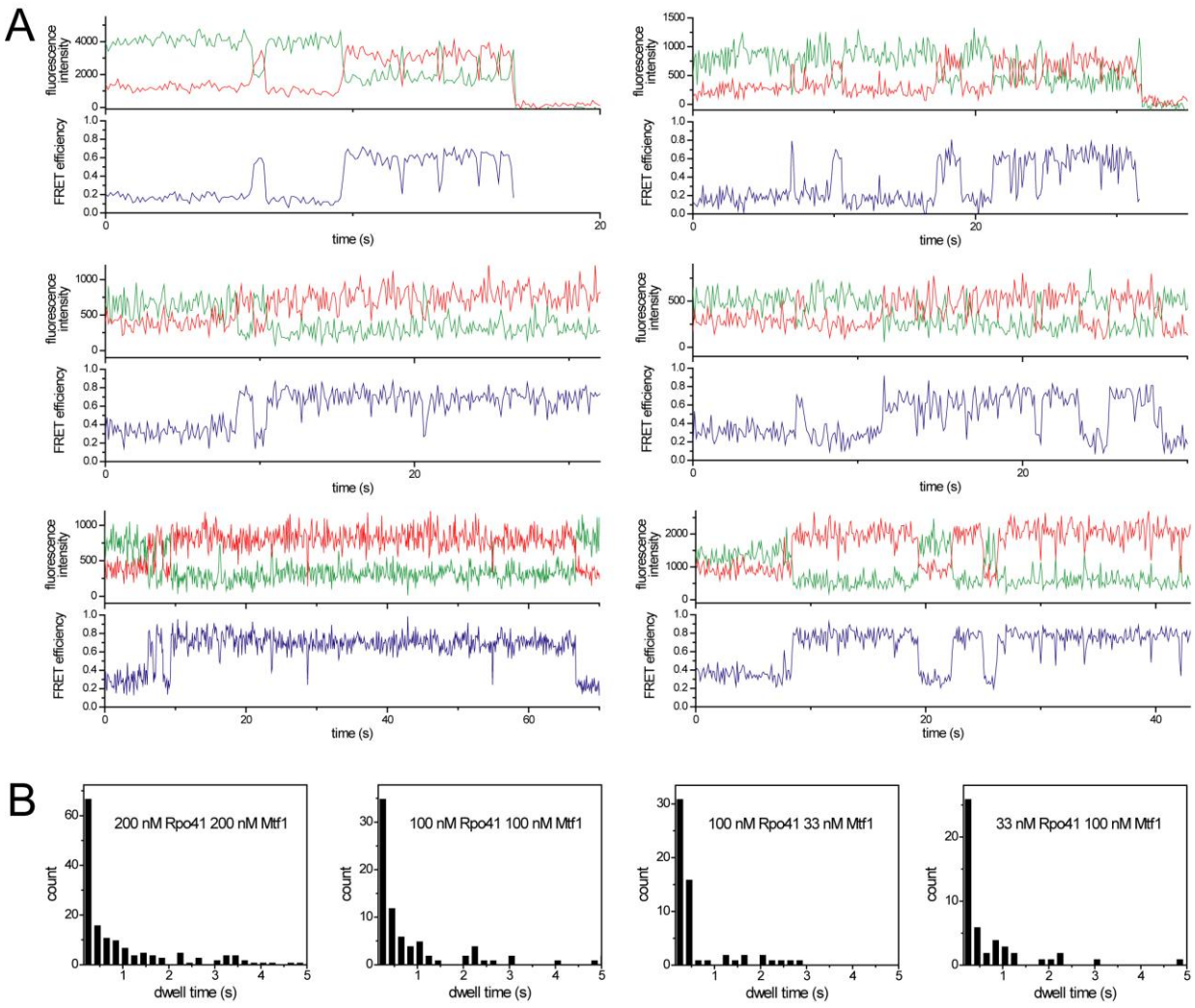

Supplementary Figure S9. Examples of initial opening trials and the dependence of the initial promoter opening interval on the protein concentration

(A) Examples of flow-in traces showing distinct initial opening trials.

(B) Lifetime distribution of the first closed state, t_2 in Figure 4c, at various concentrations of the proteins.